




COM902, a novel therapeutic antibody targeting TIGIT augments anti-tumor T cell function in combination with PVRIG or PD-1 pathway blockade

Kyle Hansen¹ · Sandeep Kumar¹ · Kathryn Logronio¹ · Sarah Whelan¹ · Samir Qurashi¹ · Hsin-Yuan Cheng¹ · Andrew Drake¹ · Margaret Tang¹ · Patrick Wall¹ · David Bernados¹ · Ling Leung¹ · Eran Ophir²  · Zoya Alteber² · Gady Cojocar² · Moran Galperin² · Masha Frenkel² · Mark White¹ · John Hunter¹ · Spencer C. Liang¹ · Maya F. Kotturi¹

Received: 13 September 2020 / Accepted: 22 March 2021 / Published online: 26 April 2021
© The Author(s), under exclusive licence to Springer-Verlag GmbH Germany, part of Springer Nature 2021

Abstract

Immune checkpoint inhibitors (ICIs) have emerged as promising therapies for the treatment of cancer. However, existing ICIs, namely PD-(L)1 and CTLA-4 inhibitors, generate durable responses only in a subset of patients. TIGIT is a co-inhibitory receptor and member of the DNAM-1 family of immune modulating proteins. We evaluated the prevalence of TIGIT and its cognate ligand, PVR (CD155), in human cancers by assessing their expression in a large set of solid tumors. TIGIT is expressed on CD4⁺ and CD8⁺ TILs and is upregulated in tumors compared to normal tissues. PVR is expressed on tumor cells and tumor-associated macrophages from multiple solid tumors. We explored the therapeutic potential of targeting TIGIT by generating COM902, a fully human anti-TIGIT hinge-stabilized IgG4 monoclonal antibody that binds specifically to human, cynomolgus monkey, and mouse TIGIT, and disrupts the binding of TIGIT with PVR. COM902, either alone or in combination with a PVRIG (COM701) or PD-1 inhibitor, enhances antigen-specific human T cell responses in-vitro. In-vivo, a mouse chimeric version of COM902 in combination with an anti-PVRIG or anti-PD-L1 antibody inhibited tumor growth and increased survival in two syngeneic mouse tumor models. In summary, COM902 enhances anti-tumor immune responses and is a promising candidate for the treatment of advanced malignancies.

Keywords TIGIT · PVRIG · Cancer immunotherapy · Checkpoint inhibitors

Introduction

Antibodies targeting checkpoint receptors such as CTLA-4 or PD-1 have revolutionized cancer treatment. However, most patients do not derive long-term benefit from cancer immunotherapies due to primary and adaptive resistance mechanisms, and one third of treated patients relapse by developing acquired resistance [1]. Therefore, targeting of additional immune-suppression mechanisms to overcome resistance to current immunotherapies may provide therapeutic benefit. Members of the DNAM-1 family that interact with nectin and nectin-like molecules have recently emerged as important regulators of tumor immune surveillance. Several members of the DNAM-1 axis are under preclinical and clinical investigation as targets for novel immunotherapies, including: TIGIT (T cell Ig and immunoreceptor tyrosine-based inhibitory motif [ITIM] domain), CD96, and PVRIG (poliovirus receptor related Ig domain containing protein). TIGIT and PVRIG are non-redundant inhibitory receptors within the same biological axis, with TIGIT being the high affinity, functional receptor for PVR, whereas PVRIG is the dominant functional receptor for PVRL2 (CD112) [2]. TIGIT is an inhibitory receptor on T and NK cells [3, 4] that competes for PVR binding with the co-activatory receptor DNAM-1 (CD226) [4–7]. PVRIG was recently identified as a co-inhibitory functional receptor expressed on NK and T cells in the tumor microenvironment (TME) [2, 8] that competes for PVRL2 binding with the co-activatory receptor DNAM-1.

✉ Eran Ophir
Erano@cgen.com

¹ Compugen USA, Inc, South San Francisco, CA, USA

² Compugen Ltd, Azrieli Center, 26 Harokmim St. Bldg D, 5885849 Holon, Israel

A Phase 1 clinical trial is currently underway to assess the safety and tolerability of a first-in-class therapeutic antibody targeting PVRIG (COM701) as a monotherapy and in combination with the PD-1 inhibitor, nivolumab, in patients with advanced solid tumors [9].

Several studies have shown that TIGIT is a marker of T cell dysfunction and is upregulated on human viral-specific CD8⁺ T cells and tumor infiltrating T cells (TILs). In a murine model of chronic viral infection, TIGIT was found to be co-expressed with PD-1 on CD8⁺ T cells, and synergistic inhibition of TIGIT and PD-1 increased viral clearance and T cell effector function [10]. Similarly, in murine models of colon and breast carcinomas, anti-TIGIT and anti-PD-L1 antibody treatment resulted in tumor rejection, an effect that was shown to be CD8⁺ T cell dependent [10]. In human settings, TIGIT blockade either alone or in combination with anti-PD-1 synergistically increased effector function of NY-ESO-1-specific CD8⁺ TILs isolated from melanoma patients [11]. Collectively, these data suggest that TIGIT and PD-1/PD-L1 co-blockade acts through CD8⁺ T cells to generate an effective anti-tumor immune response.

Currently, numerous antagonist TIGIT antibodies are in preclinical and clinical development to treat patients with locally advanced or metastatic tumors [12, 13]. These early clinical studies have begun to shed light on whether TIGIT checkpoint inhibitors, either as a single agent or in combination with other cancer therapies, will generate durable responses in patients who do not benefit from anti-PD-1/PD-L1 therapies. Phase 1 studies to date have shown only limited responses for TIGIT inhibitors, either alone or in combination with anti-PD-1/PD-L1 antibodies [14–16]. However, the recent Phase 2 CITYSCAPE trial in non-small cell lung cancer (NSCLC) demonstrated a clear benefit of combining tiragolumab with atezolizumab relative to treatment with atezolizumab alone [17]. Given the isotype differences between the antibodies in development [effector human IgG1 (hIgG1) versus non-effector such as hIgG4 or Fc-silenced hIgG1], these studies may also determine whether isotype influences the immune response developed upon anti-TIGIT therapy. The majority of the clinical data reported thus far has been with anti-TIGIT hIgG1 isotypes (etigilimab, tiragolumab, and vibostolimab). A Phase 1 study was also completed with ASP8374, an anti-TIGIT hIgG4 isotype, in Japanese patients with advanced solid tumors. However, a Phase 1b study of ASP8374 as a single agent and in combination with pembrolizumab was halted in October 2020 by Astellas for undisclosed reasons. In contrast, an anti-TIGIT antibody with a mutated hIgG1 to reduce Fc γ receptor binding (domvanalimab, Arcus Biosciences), is currently being evaluated in a randomized Phase 2 study in combination with anti-PD-1 alone or with etrumadenant, a dual A2a/A2b adenosine receptor antagonist (NCT04262856). Moreover, the evaluation of domvanalimab in combination

with anti-PD-1 has been expanded to a Phase 3 trial in PD-L1-positive, locally advanced, or metastatic non-small cell lung cancer patients (NCT04736173).

COM902 is a novel, fully human anti-TIGIT hinge-stabilized IgG4 monoclonal antibody (mAb) that specifically binds TIGIT with high affinity and disrupts its interaction with the cognate ligand, PVR. TIGIT targeting combined with PVRIG or PD-1 pathway blockade represents a strategy for improving efficacy in patients that develop resistance or do not respond to PD-1/PD-L1 blockade alone.

Materials and methods

Antibodies

COM902 is a fully human anti-TIGIT IgG4 isolated by panning a phage display antibody library (XOMA Corp.) with human TIGIT (hTIGIT) ECD. COM902 was optimized for improved affinity and cross-reactivity by saturation mutagenesis in the H-CDR2 and L-CDR3. COM701 is a humanized anti-PVRIG IgG4 mAb and was described previously [2]. Pembrolizumab, anti-PD-L1 mouse IgG1 (mIgG1, Clone YW243.55.S70), and isotype control antibodies were produced internally [18]. Chimeric COM902 contains the human variable chains of COM902 and the constant region of mIgG1. Anti-mouse PVRIG (mPVRIG) mIgG1 was described previously [19].

Tumor processing and flow cytometry

Human tumor samples were acquired from the Cooperative Human Tissue Network (CHTN). The tumor and histological type were determined from the pathology report (Supplementary Table S1). Lineage marker and isotype control antibodies are presented in Supplementary Table S2. Samples were acquired on a Fortessa X-20 cytometer (BD Biosciences). Data were analyzed using FlowJo (TreeStar LLC) with the gating lineages defined in Supplementary Table S3.

KinExA

Kinetic exclusion assay (KinExA 3200 instrument, Sapi-dyne Instruments) was used to measure hTIGIT (Sino Biologicals) binding to COM902. Six total binding curves were acquired with [hTIGIT] = 854–588 pM equilibrated for ~72 h with [COM902]_{binding sites} = 1.1–5.7 pM and ~24 h with [COM902]_{binding sites} = 28.7 pM at 22 °C. All six curves were simultaneously fit to a 1:1 equilibrium model using the KinExA software to estimate K_D . Detection beads were hTIGIT coupled to Ultralink Support resin (Thermo

Scientific), and the secondary detection antibody was AF647-labeled goat anti-human IgG, Fc-fragment specific (Jackson ImmunoResearch Laboratories, West Grove, PA).

Immunohistochemistry

Expression of hPVR in human formalin fixed paraffin embedded (FFPE) tissues was evaluated using an anti-hPVR rabbit mAb (Clone D8A5G; Cell Signaling Technologies). Immuno-histochemistry (IHC) staining was conducted using an IntelliPATH™ automated staining platform (Biocare). Human PVR expression in FFPE tissue microarray (TMA) samples was scored by a pathologist on a quantitative scale based on the percentage of positive cells, and the completeness and intensity of the cell membrane staining (Supplementary Figure S1f). Halo software (Indica labs) was used for digital image analysis (OracleBio, Scotland, UK).

TIGIT binding and blocking assays

ExPi293 cells were engineered to express hTIGIT, cynomolgus TIGIT (cTIGIT), or mouse TIGIT (mTIGIT). For binding experiments, cells were incubated for 1 h with COM902 or hIgG4 isotype control and detected with a secondary antibody. For blocking experiments, the cell lines described above were pre-incubated with COM902 or hIgG4 isotype for 30 min. Recombinant hPVR-mIgG2a-Fc (hPVR-Fc) and cynomolgus PVR-hIgG1-Fc-biotin (cPVR-Fc) produced internally, or mouse PVR-hIgG1-Fc (mPVR-Fc) (Sino Biological) were added to the cells for 1 h and detected with fluorescently labeled secondary antibodies. The fluorescent signal was detected by flow cytometry and corresponded to the % of PVR blocking to cell-surface expressed TIGIT.

CDC and ADCC assays

For complement dependent cytotoxicity (CDC), 5% baby rabbit serum containing complement (Cedarlane) was added to activated human CD8⁺ T cells. COM902, hIgG4 isotype, Campath (anti-human CD52 hIgG1), or hIgG1 isotype were added and cell lysis was measured using a Cytotox-Glo reagent kit (Promega). For ADCC assays, activated human CD8⁺ T cells were labeled with DELFIA BATDA reagent (Perkin Elmer) and combined with activated NK cells. The same antibodies as used for the CDC assay were added. Time resolved fluorescence (TRF) signal was detected after 4 h of incubation using an EnVision multi-label reader (Perkin Elmer).

Jurkat reporter assay

Jurkat cells were engineered to express hTIGIT and a luciferase reporter driven by an IL-2 response element (Jurkat

hTIGIT-IL-2) (Promega, TIGIT/CD155 Blockade Bioassay). Jurkat hTIGIT-IL-2 cells were cultured with CHO-K1 cells engineered to express human CD155 (hPVR) and a TCR activating complex (CHO-K1 hPVR-TCR). COM902 or hIgG4 isotype were added to the co-culture and luminescence was quantified on an EnVision multi-label reader (Perkin Elmer).

CMV CD8⁺ T cell co-culture assay

Human CMV pp65_(495–503) reactive CD8⁺ T cells were expanded by thawing peripheral blood

mononuclear cells (PBMCs) from CMV seropositive donors (CTL). PBMCs were cultured for eight days with recombinant human IL-2 (rhIL-2) and rhIL-7, and replenished at days 3 and 5. At day 8, cells were harvested, and cultured in low dose rhIL-2 (100 U/mL) at 2×10^6 cells/mL in complete RPMI media for 2–3 days. The frequency CMV pp65_(495–503) reactive CD8⁺ T cells was determined with iTag Tetramer—HLA-A*0201 CMV pp65 (NLVPM-VATV) (MBL-Bion) staining [2]. The resulting CMV⁺ antigen-specific CD8⁺ T cells were $\geq 90\%$ CMV pp65-tetramer positive. CMV antigen-specific T cells were co-cultured for 18 h with Mel-624 (ATCC) cells that were engineered to over-express the CMV peptide pp65_(495–503).

A human IFN- γ flex cytokine bead assay kit (BD Biosciences) was used to detect secreted IFN- γ in the cell culture supernatant. For anti-PD-1 combination assays, the Mel-624 cells were engineered to overexpress human PD-L1 and the CMV protein pp65_(495–503) using lentiviral transduction. For T-cell mediated cell killing, Mel-624 cells were engineered to over-express human PVR, PVRL2, and firefly luciferase (Mel-624-PVR-PVRL2-luc). Mel-624 cells were pulsed with pp65_(495–503) peptide for 1 h and combined with CMV-specific CD8⁺ cells. Bio-Glo luciferase substrate (Promega) was added after 16 h according to the manufacturer's instructions. Luminescence was detected using an EnVision multi-label reader (Perkin Elmer).

NK cell cytotoxicity assay

Purified human NK cells were cultured for 16 h with rhIL-15 (R&D systems) then added to a co-culture with CAL-27 cells (ATCC) at a 10:1 E:T ratio for 4 h in the presence of COM701, COM902 (10 μ g/mL each), COM701 + COM902, or a hIgG4 isotype control. NK cell cytotoxicity was measured by the expression of CD107a on NK cells.

OVA-specific mouse CD8⁺ T cell co-culture assay

Ovabumin (OVA)-specific CD8⁺ T cells were generated from the spleens of female C57BL/6-Tg (Tcr α Tcr β)1100Mjb/J mice (OT-1, The Jackson Laboratory). Splenocytes were

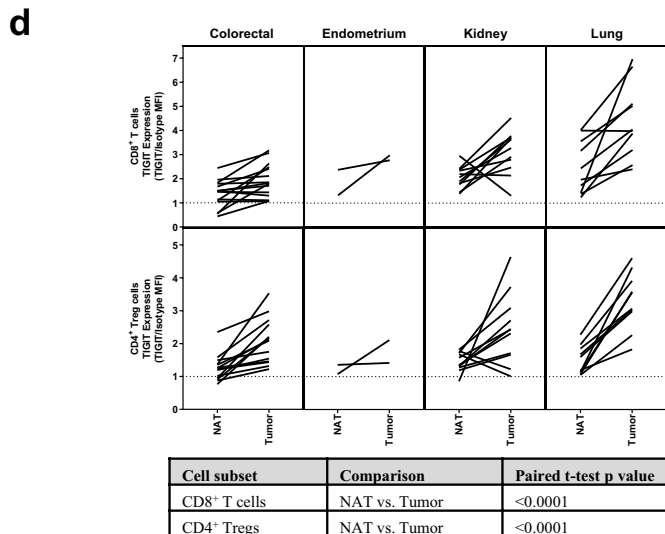
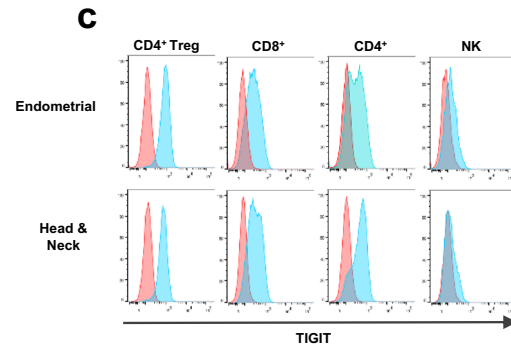
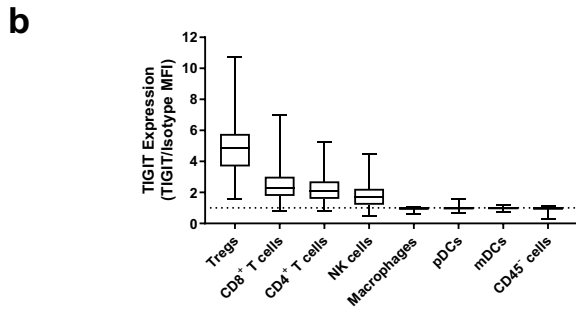
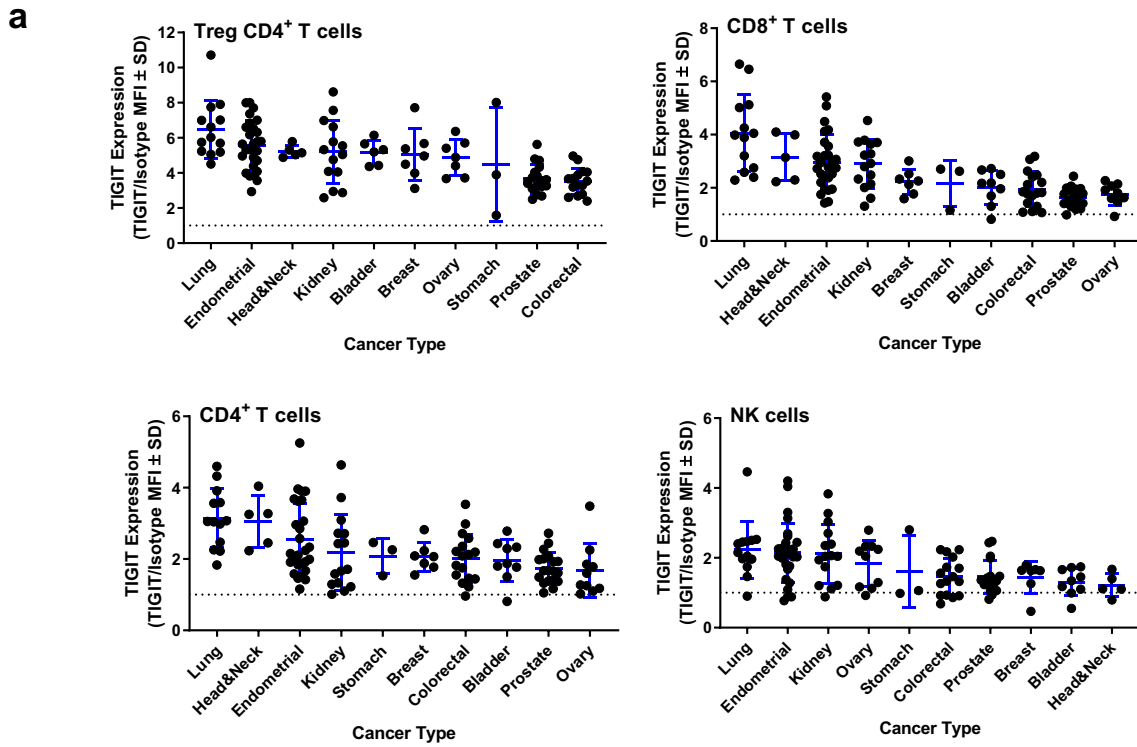


Fig. 1 Expression of TIGIT on cells isolated from dissociated tumors and NATs. **a** TIGIT expression is shown on Treg CD4⁺ T, CD8⁺ T, non-Treg CD4⁺ T, and NK cells for each tumor type. Each dot within a column represents an individual sample. Mean ± SEM is presented. **b** Across all tumor samples examined, the expression of TIGIT on the different cell types is shown. The median is depicted by the middle line and the upper and lower quartiles are depicted by the boxes above and below the median line. The whiskers depict 1.5 times the interquartile range. **c** Representative histograms for TIGIT expression (blue) compared to an isotype control (red) are shown for four lymphocyte subsets isolated from an endometrial and a head and neck tumor. **d** Matched tumor and NAT samples were assessed for TIGIT expression on CD8⁺ T cells and CD4⁺ Tregs. Each line represents a matched donor

stimulated for 48 h with 1 µg/mL H-2 Kb-restricted OVA peptide (SIINFEKL, Anaspec) and rhIL-2. MC38 cells were pulsed with OT-1 peptide and combined with OVA-specific CD8⁺ T cells. Chimeric COM902, anti-PD-L1, mIgG1 or rat IgG2b (rIgG2b) isotype controls were added and plates were incubated for 24 h. Mouse IFN-γ was measured using a mouse IFN-γ Flex Set Kit (BD Biosciences).

Syngeneic mouse tumor models

5×10^5 CT26 cells or 1×10^6 Renca cells (ATCC) were inoculated subcutaneously into the right flank of female Balb/c mice. Mice with tumors measuring 20–55 mm³ were randomized (into groups of 10 mice). Antibodies were administered through intraperitoneal injection on day 6 (monotherapy) or day 8 (combination therapy) post tumor inoculation and dosed three times a week for two weeks. Chimeric COM902 and anti-mPVRIG were titrated in the CT26 model to select the saturating dose of 10 mg/kg. Anti-PD-L1 was similarly titrated, and the dose of 3 mg/kg was selected to accentuate the effect of combination treatment on tumor growth. Mice were euthanized when the tumor volumes reached 2000 mm³. To isolate TILs, CT26 tumors were dissociated with GentleMACs™ kits (Miltenyi Biotec). Lineage marker and isotype control antibodies used are listed in Supplementary Table S5. Gating lineages are described in Supplementary Table S5. All animals were housed during the study in an internal animal facility with food and water provided, ad libitum. All studies were approved by the Institutional Animal Care and Use Committee at the Compugen USA, Inc.

Statistics and calculations

The “log (agonist) vs. response—variable slope (four parameters)” model in Prism was used to model dose–response data from in-vitro functional assays. Data were analyzed by paired Student t test; *, $P < 0.05$; **, $P < 0.01$; ***, $P < 0.001$. Estimates of the half maximal inhibitory concentration (IC₅₀) or half maximal effective concentration (EC₅₀) were calculated

based on these models. The percentage of specific cytotoxicity was calculated as: $(1 - (\text{RLU}_{(\text{target cells} + \text{T cells} + \text{antibody})} / \text{RLU}_{(\text{target cells} + \text{T cells} + \text{media alone})})) \times 100$. For in-vivo studies, two-way ANOVA with repeated measures for selected pairs of groups was performed using JUMP software (Statistical Discoveries™). Tumor growth inhibition (TGI) at termination was performed by comparing tumor volumes measured on the last day on which all study animals were alive. Statistical differences in survival were determined by Log-rank P-value associated with each set of Kaplan–Meier curves.

Results

TIGIT is expressed and induced in solid tumors

Although TIGIT protein expression has been examined on TILs in small subsets of human tumors [10, 11, 20, 21], expression across a large number of cancers with multiple tumors per indication has not been investigated. Thus, to further examine TIGIT in the TME, we assessed expression in ~130 unique dissociated human tumors from 10 different cancer indications. Since CD127 expression is inversely correlated with Foxp3 expression, CD4⁺ regulatory T cells (Tregs) were defined as CD4⁺CD25⁺CD127⁻ [22]. TIGIT expression was detected on Tregs, CD8⁺ T cells, non-Treg CD4⁺ T cells, and NK cells from multiple tumor types (Fig. 1a). Across all tumors, TIGIT was expressed, from highest to lowest, on Tregs, CD8⁺ T cells, non-Treg CD4⁺ T cells, and NK cells (Fig. 1b, c). TIGIT expression was higher on CD4⁺ Treg and CD8⁺ T cells derived from tumor tissue compared to matched normal adjacent tissue (NAT) (Fig. 1d). No TIGIT expression was detected on monocytes, dendritic cells (DCs), or non-immune cells (Fig. 1b). Across all examined indications, lung, endometrium, head and neck, and kidney cancers had the highest TIGIT expression for all lymphocyte subsets evaluated (Fig. 1a). As CD8⁺ T and NK cells are known to be important cytotoxic lymphocytes within the immune system, high TIGIT expression on these cell types suggests that TIGIT plays a critical role in regulating their activity.

PVR is expressed in multiple tumor types

A subset of samples that were evaluated for TIGIT expression were also examined by flow cytometry for PVR expression. PVR expression was detected on two major cell subsets: 1) myeloid cells, and 2) non-immune CD45⁻ cells, (Supplemental Figure S1a–d). Significant correlations between the prevalence of TIGIT versus PVR expression could not be generated due to sample size limitations. PVR expression was also evaluated in FFPE tissues by IHC. Ten non-small cell lung cancer (NSCLC), small-cell lung cancer

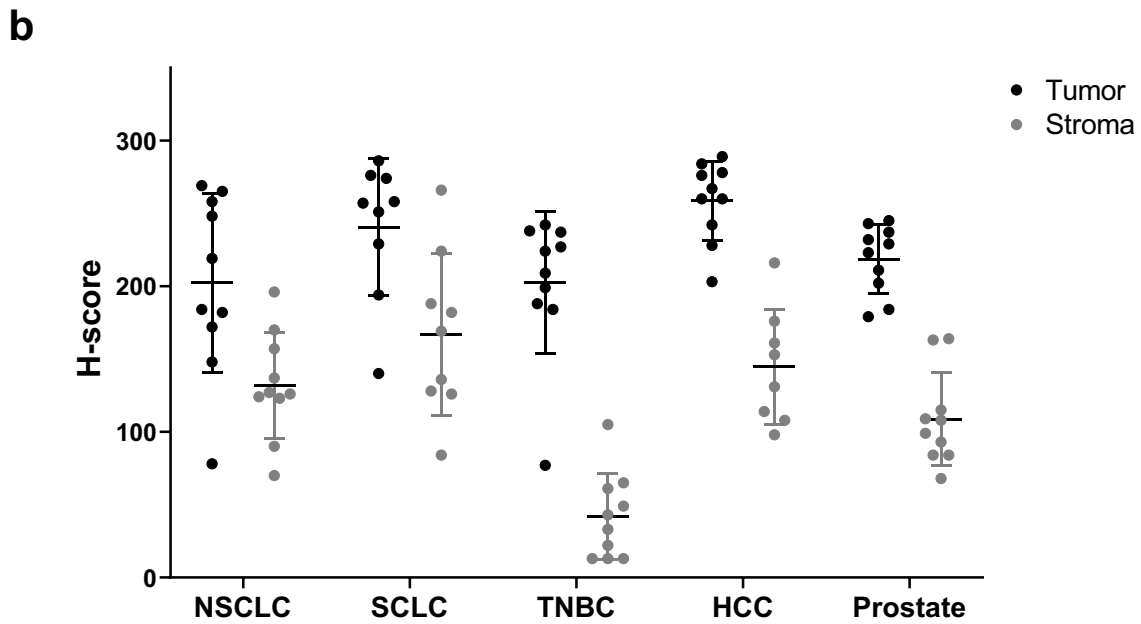
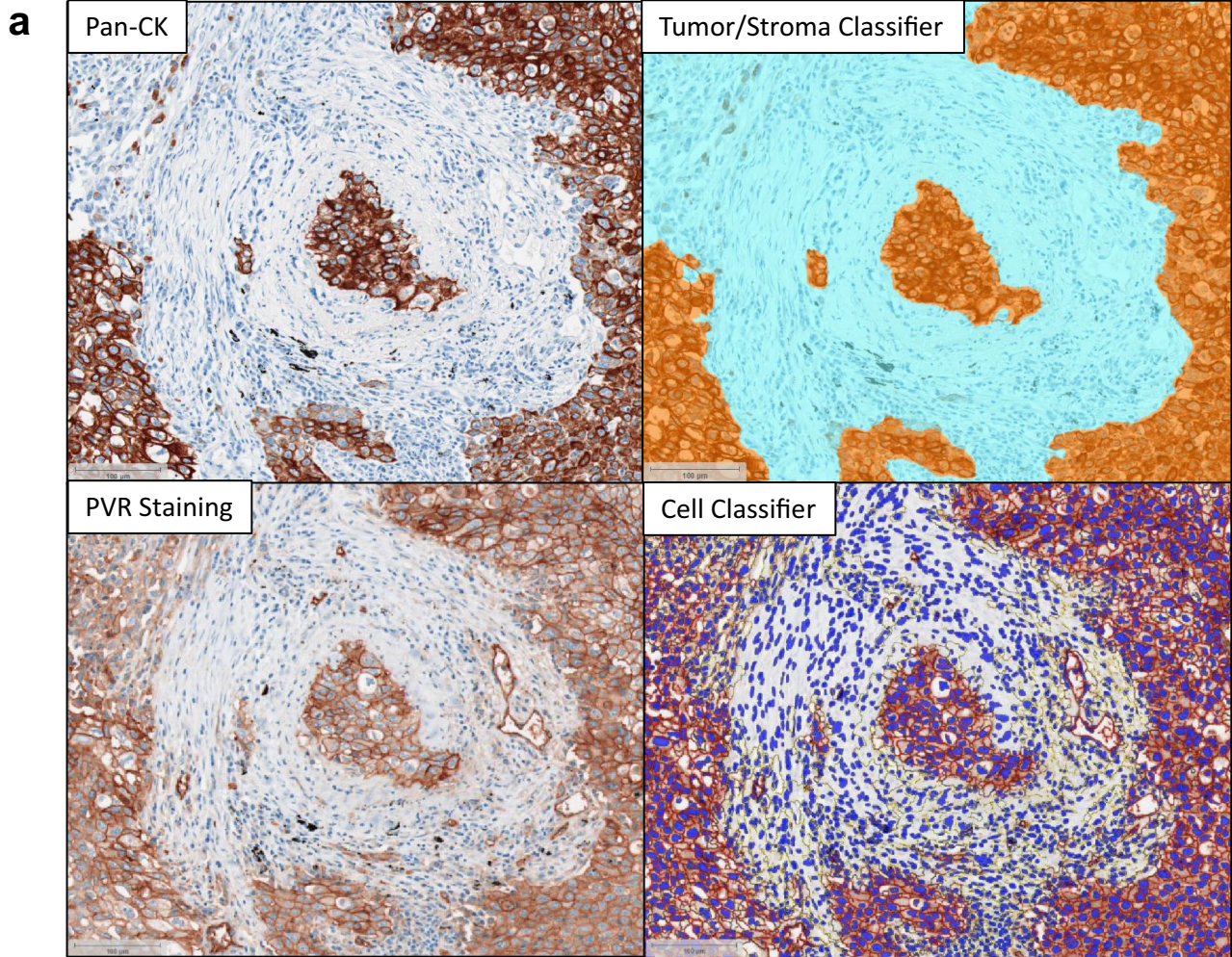


Fig. 2 Expression of PVR in the TME. **a** Representative images from digital image analysis of PVR IHC staining in a lung tumor. Staining of Pan-CK and PVR was carried out on serial sections from FFPE tumor samples. Top left: Pan-CK tumor marker staining. Top right: Tumor/stroma boundary classifier. Bottom left: PVR staining within the tumor and adjacent stroma. Bottom right: Cell identification and membrane expression classifier. **b** Summary of PVR H-score values from the tumor and stroma of 10 NSCLC, SCLC, TNBC, HCC, and prostate FFPE tumor samples. Each dot represents an individual sample, with tumor expression in black and stroma expression in gray. Mean \pm SEM is presented

(SCLC), triple negative breast cancer (TNBC), hepatocellular cancer (HCC), and prostate cancer tumors were stained with anti-hPVR and pan-cytokeratin (Pan-CK). Using a novel digital image analysis for scoring PVR expression, the tumor/stromal border, cell segmentation, and membrane versus cytoplasmic staining delineation were determined (Fig. 2a). All five tumor types had high PVR expression, with H-scores ranging from 80 to 280 (Fig. 2b). Across all tumor types examined, PVR expression was higher in the tumor compartment compared to the stromal area (Fig. 2b). As PVR expression was highest on malignant cells, we further evaluated PVR expression on a panel of TMAs from 15 tumor types. PVR expression was scored using a 0, 1, 2, or 3 scoring system (Supplemental Figure S1e and S1f). PVR was detected in multiple tumor types, with the highest expression in colon cancer samples (Supplemental Figure S1g).

COM902 binds to TIGIT and blocks TIGIT:PVR interactions

The binding affinity of COM902 to TIGIT was characterized by both a cell-based antibody binding assay and kinetic exclusion (KinExA). COM902 bound with similar high affinity to hTIGIT and cTIGIT expressed on cells, while much lower binding affinity was observed for mTIGIT (Fig. 3a, Supplemental Figure S2a). Binding of COM902 to hTIGIT expressed on the cell surface yielded K_D values ranging from 0.11 to 0.3 nM. Binding of COM902 to a monomeric recombinant hTIGIT protein using KinExA yielded a K_D value of 626 fM (Supplemental Figure S2b).

Given the low affinity interaction and questionable biological relevance of TIGIT binding to PVRL2 and PVRL3 [2–4], we focused on the ability of COM902 to block the interaction of TIGIT with its high-affinity ligand, PVR. We utilized a cell-based blocking assay in which TIGIT was expressed on the cell surface and PVR was added as a recombinant protein. COM902 showed complete inhibition of the human and cynomolgus TIGIT:PVR interaction, with IC_{50} 's of 0.18 ± 0.02 nM and 0.55 ± 0.03 nM, respectively (Fig. 3b, Supplemental Figure S2a). Additionally, we assessed ability of a chimeric COM902 mIgG1 to block

the mouse TIGIT:PVR interaction. The chimeric antibody blocked the interaction of mPVR-Fc to mTIGIT with an IC_{50} of 0.16 ± 0.03 nM. Taken together, these data suggest that COM902 shares a similar mechanism of action across human, cynomolgus monkey and mouse.

COM902 does not demonstrate ADCC or CDC activity

TIGIT is highly expressed on $CD8^+$ TILs which are important mediators of the anti-tumor immune response [23]. Since depletion of TIGIT⁺ lymphocytes would be an undesirable outcome of COM902 on-target binding, we assessed whether COM902 could mediate Fc-dependent CDC or ADCC against TIGIT⁺ T cells. For CDC assessment, activated TIGIT⁺ human T cells were incubated with complement-containing baby rabbit serum. COM902, or anti-CD52 (Campath) was added to the culture, and the amount of cell lysis was determined. COM902 did not mediate CDC whereas Campath mediated CDC in a dose-dependent manner (Fig. 4a). To assess ADCC activity, activated TIGIT⁺ human T cells were co-cultured with activated human NK cells. In contrast to Campath, which induced ADCC in a dose-dependent manner, COM902 did not demonstrate ADCC activity (Fig. 4b).

COM902 enhances human lymphocyte function in-vitro

To evaluate the functional effect of TIGIT:PVR interaction blockade by COM902, we utilized a Jurkat luciferase reporter co-culture system. CHO-K1 cells expressing anti-CD3 (OKT3) and hPVR (CHO-K1-OKT3-PVR⁺) were incubated with Jurkat-TIGIT-IL-2-luc reporter cells. As shown in Fig. 5a, blockade of TIGIT:PVR by COM902 increased luciferase production, with an EC_{50} of 2.14 nM. Next, we evaluated the effect of COM902 on antigen-specific T cell function using a peptide re-stimulation assay. PBMCs were activated with a viral pp65_(495–503) antigen peptide and CMV-reactive effector $CD8^+$ T cells were assessed for TIGIT, PVRIG, and PD-1 expression (Fig. 5b). CMV-specific $CD8^+$ T cells (Supplemental Figure S2c) were co-cultured with a PVR⁺ cancer cell line ectopically expressing the pp65 protein (Mel-624-pp65) (Fig. 5b). COM902 significantly increased IFN- γ secretion for all three donors tested (Fig. 5c). Since a primary function of effector $CD8^+$ T cells in the TME is cytotoxic cell killing, we modified the re-stimulation assay to evaluate this readout. Mel-624 cells engineered to ectopically express firefly luciferase, were pulsed with pp65_(495–503) peptide and co-cultured with CMV-specific $CD8^+$ T cells. COM902 increased the specific cell killing of Mel-624 in a dose-dependent manner, with an EC_{50} of 0.01 ± 0.05 nM (Fig. 5d). Interestingly, there was

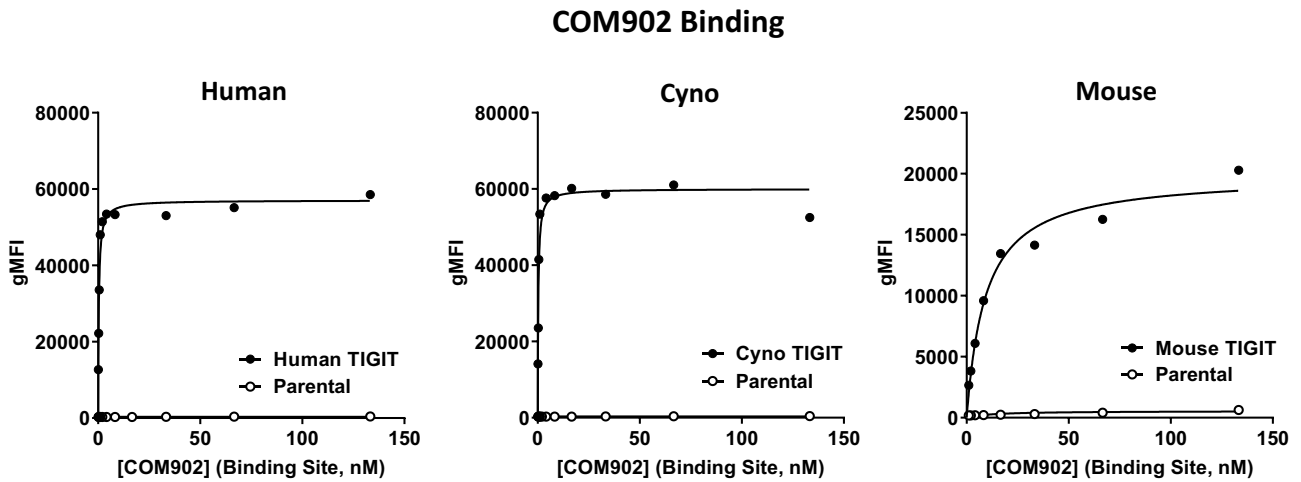
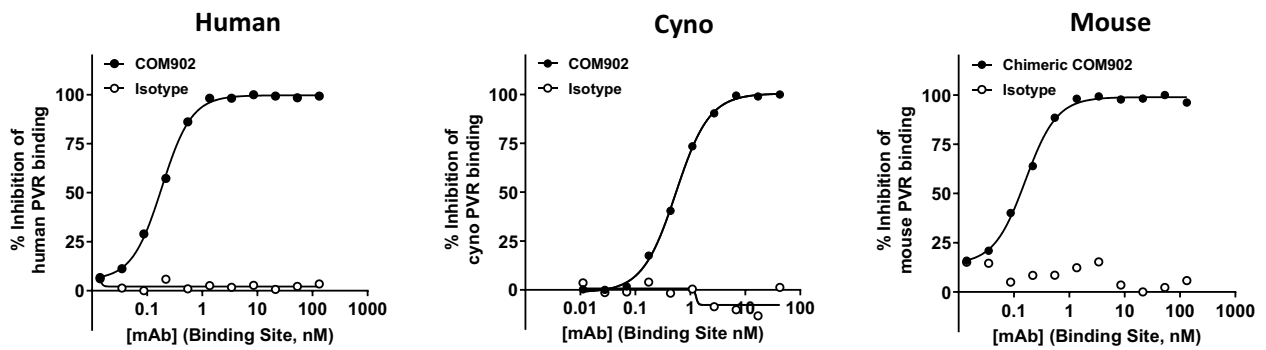
a**b****COM902 Receptor-Ligand Blocking**

Fig. 3 COM902 binds specifically to TIGIT and blocks TIGIT:PVR binding. **a** Binding of COM902 to human, cynomolgus, and mouse TIGIT over-expressing cells and non-expressing parental cells. **b**

Assessment of the ability of COM902 and chimeric COM902 to block the interaction of TIGIT and PVR. Concentrations shown on x axis are total binding site concentration in nM

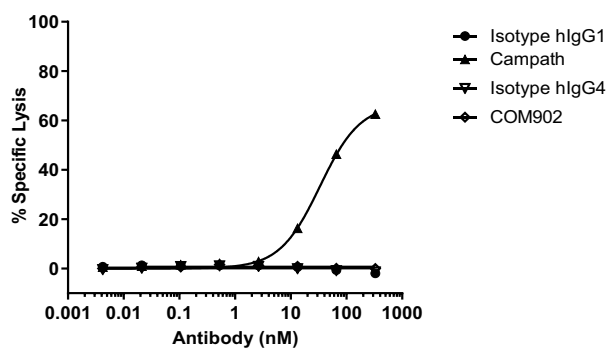
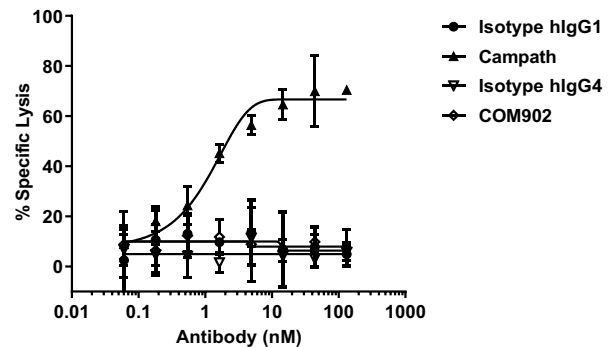
a**b**

Fig. 4 COM902 does not induce ADCC or CDC activity. **a** ADCC activity assessment for COM902. **b** CDC activity assessment for COM902. Campath (anti-CD52) hIgG1 was used as a positive control. Representative data from $n \geq 2$ is shown for each graph

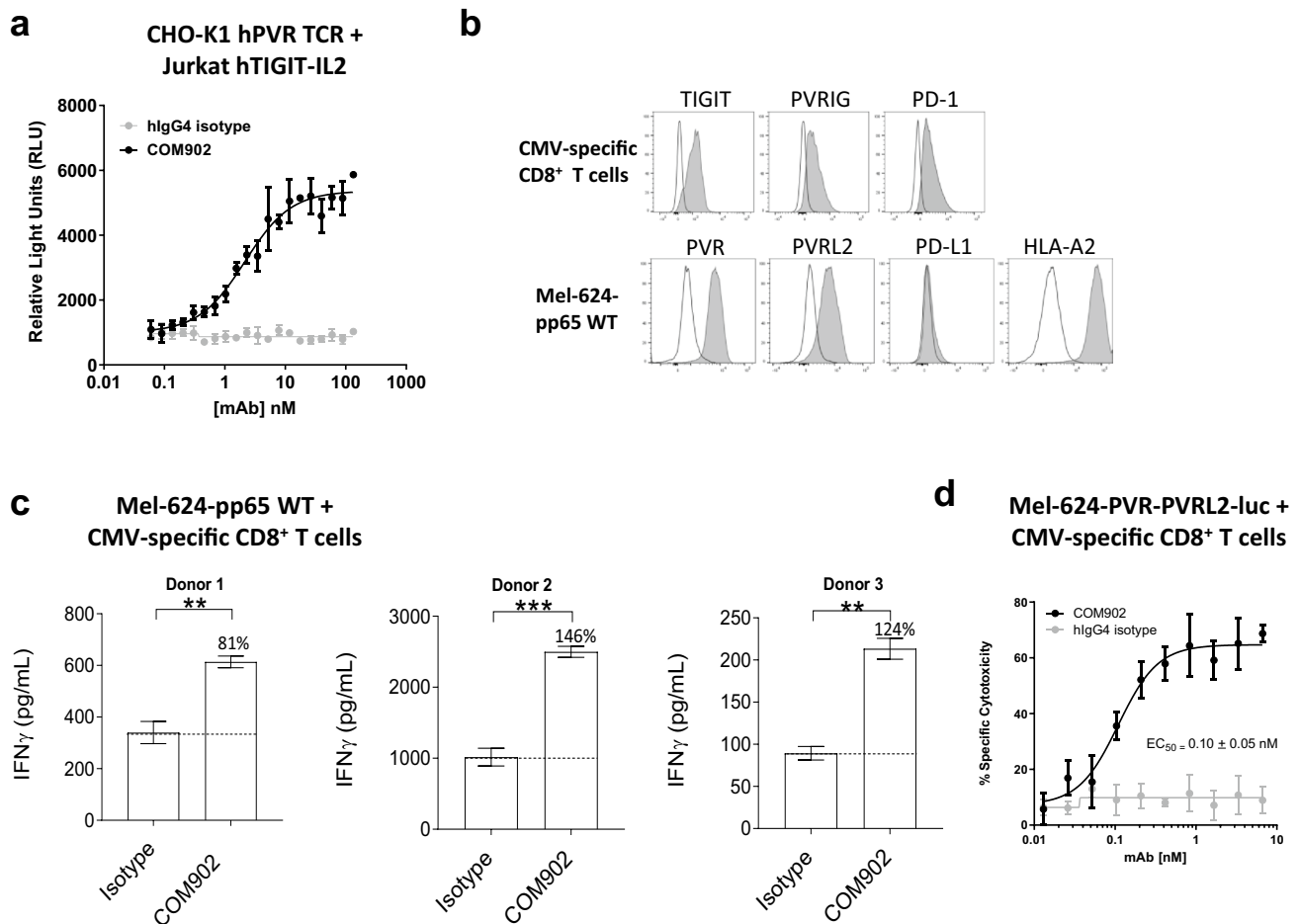


Fig. 5 COM902 enhances human T cell function. **a** COM902 increases IL-2 signaling. Representative data ($n \geq 2$) shows the RLU (mean \pm SD) of the luciferase signal from a 6 h co-culture of Jurkat IL-2-RE luciferase human TIGIT cells and CHO-K1 human PVR cells. A 20 point, 1.5-fold dilution series starting at 133 nM was used for each antibody. **b** The expression of PD-1, PVRIG and TIGIT on CMV-reactive CD8⁺ T cells (top row, $n = 3$ donors), and of PVR, PVRL2, PD-L1, and HLA-A2 on Mel-624-pp65 was assessed. White histograms represent the isotype control staining, and gray represents the expression of the target of interest. **c** CMV-reactive CD8⁺ T cells were co-cultured with Mel-624-pp65

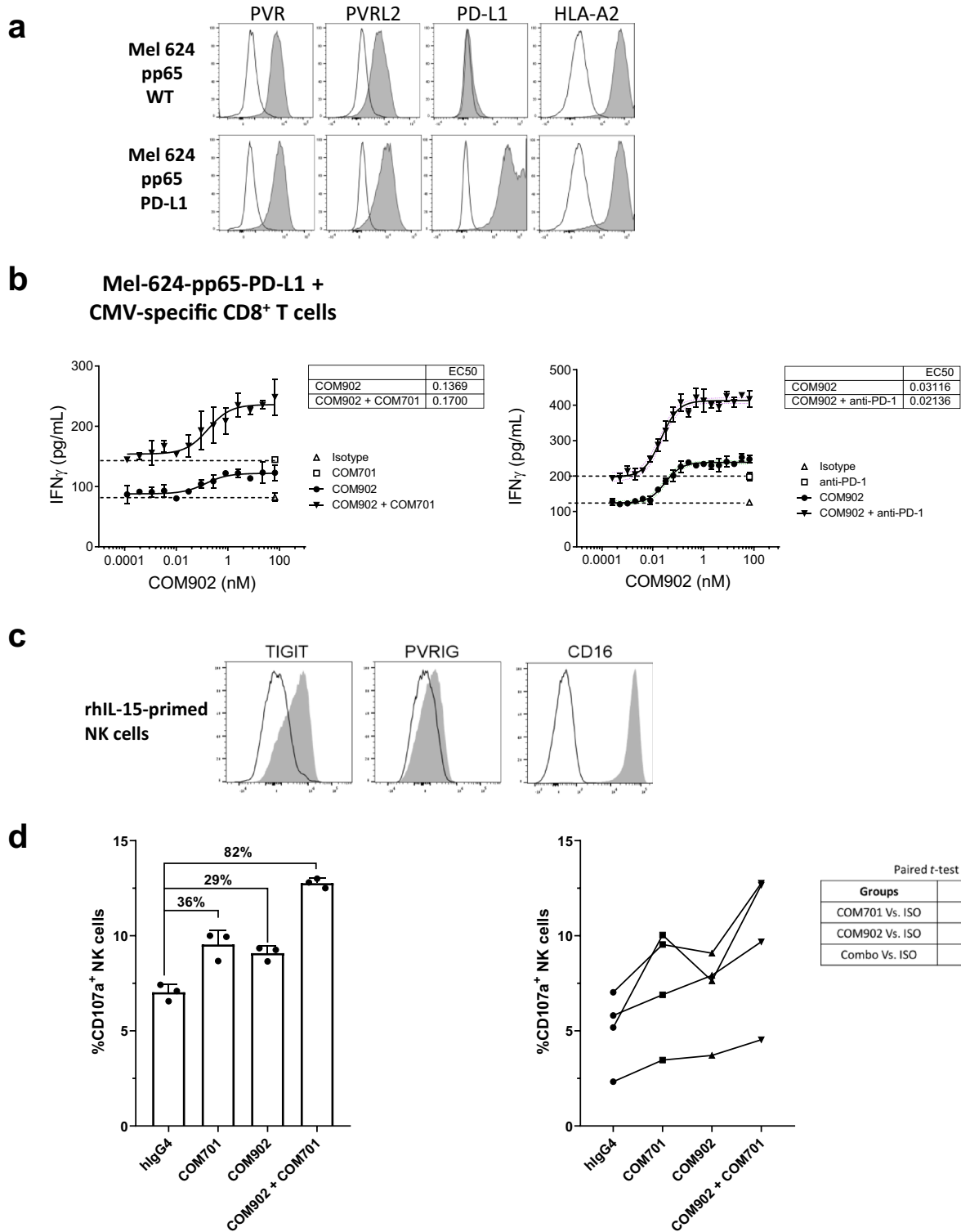
cells for 18 h in the presence of 10 μ g/mL COM902 or hIgG4 isotype control antibody. Percent change in IFN- γ for each condition relative to isotype control is depicted by the number above each bar. The bar graphs show the average \pm SD. Data were analyzed by paired Student t-test; * $p < 0.05$; ** $p < 0.01$; *** $p < 0.001$. Data shown is representative of $n \geq 3$ experiments ($n = 3$ donors). **d** CMV-reactive CD8⁺ T cells were co-cultured with CMV peptide-pulsed Mel-624 cells engineered to express hPVR, hPVRL2, and luciferase in the presence of COM902 in two-fold dose-titration range from 6.6–0.006 nM. Percent specific cytotoxicity was calculated by $(1 - (RLU_{(target\ cells+T\ cells+antibody)} / RLU_{(target\ cells+T\ cells+media\ alone)})) \times 100$

minimal killing of the Mel-624 cells with the hIgG4 isotype treatment (Fig. 5d) despite the production of IFN- γ secretion (Fig. 5c). One possibility for this difference is that the cytotoxicity assay was measured at 16 h following antibody treatment, while IFN- γ detected at 24 h.

COM902 combined with PVRIG or PD-1 pathway blockade enhances human lymphocyte function

To assess COM902 in combination with PVRIG or PD-1 blockade, CMV-reactive CD8⁺ T cells were co-cultured with Mel-624-pp65 cells and COM902 in the presence or absence of anti-PVRIG, COM701 antibody (Fig. 6a). COM902 in

a step-wise, dose-titration combined with a fixed dose of 10 μ g/mL of COM701 significantly increased IFN- γ secretion (Fig. 6b, left panel). Since Mel-624 cells express low endogenous PD-L1, we over-expressed hPD-L1 on the cell surface (Mel-624-pp65 PD-L1⁺, Fig. 6a) and co-cultured these cells with CMV-reactive CD8⁺ T cells. Similar to the synergistic effects induced by combining COM902 and COM701, a step-wise dose-titration of COM902 combined with a fixed dose of 10 μ g/mL of anti-PD-1 mAb significantly increased IFN- γ secretion compared to COM902 or anti-PD-1 alone in all tested donors (Fig. 6b, right panel). The average \pm SEM EC₅₀ value for COM902 in the presence of anti-PD-1 was 0.03 nM \pm 0.01 nM. The effects of



combining TIGIT and PVRIG blockade on NK cell cytotoxic function were also evaluated. Priming of NK cells with rhIL-15 induced the expression of CD16 and TIGIT and to a lesser extent of PVRIG (Fig. 6c). While monotherapy with COM902 or COM701 augmented NK cell activity by 36% and 29%, respectively, as measured by CD107a expression,

combination of both antibodies yielded a synergistic effect, enhancing NK cell cytotoxicity by 82% (Fig. 6d, left panel). These effects were maintained across four distinct healthy donors and were statistically significant (Fig. 6d, right panel). Collectively, these data show that blockade of TIGIT:PVR interaction by COM902 enhances lymphocyte

Fig. 6 COM902 combined with COM701 or anti-PD-1 enhances human lymphocyte function. **a** Expression of PVR, PVRL2, PD-L1, and HLA-A2 on Mel-624-pp65 parental and PD-L1 overexpressing cells. **b** COM902 was added in a 19 point, two-fold dilution series (66–0.0002 nM) in combination with either a fixed concentration of 10 µg/mL COM701, 10 µg/mL anti-PD-1 or 10 µg/mL hIgG4 isotype control to a co-culture of CMV-reactive CD8⁺ T cells and Mel-62-pp65-hPD-L1 cells. Percent change in IFN-γ relative to isotype control is shown for each condition. Graphs show representative data from two independent experiments (*n*=3 donors). **c** The expression of TIGIT, PVRIG and CD16 on rhIL-15-primed NK cells (representative example from a healthy donor). White histograms represent the isotype control staining, and gray represent the expression of the target of interest. **d** COM902, COM701, COM902+COM701 or hIgG4 isotype control mAbs were added to NK:CAL-27 cell co-cultures at 10 µg/mL. Following 4 h, CD107a cell surface expression on NK cells was analyzed by flow cytometry. A representative donor is shown in the left panel. The bar graphs show the average ± SD. NK cytotoxicity with four donors are summarized in the right panel. Data were analyzed by paired student t-test

cytokine secretion and cytotoxicity. Furthermore, this effect can be magnified by combining COM902 with blockade of other immune checkpoints, such as PVRIG and PD-1.

Chimeric COM902 combined with anti-PVRIG or anti-PD-L1 induces tumor growth inhibition

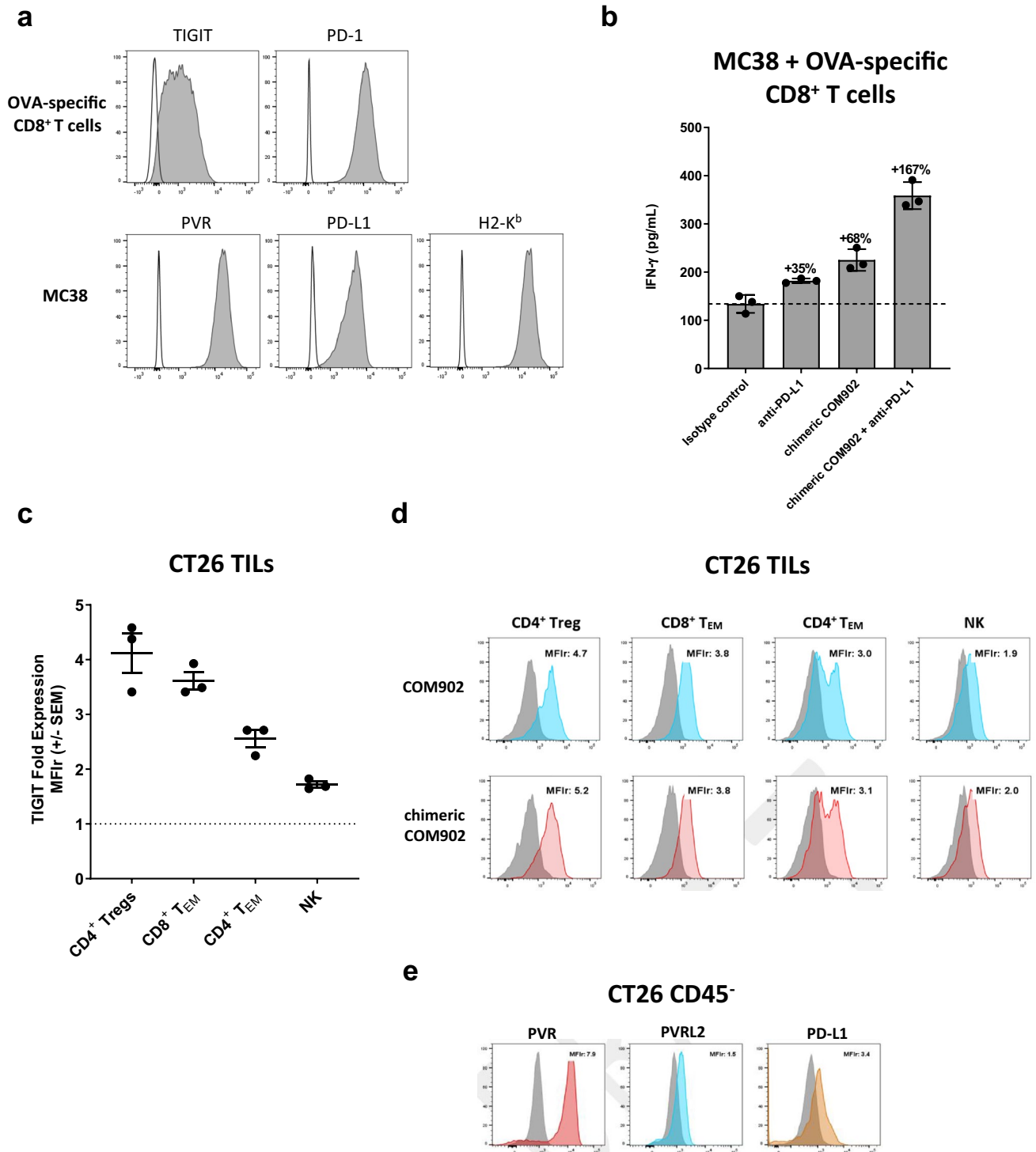
To determine if chimeric COM902 maintained similar functionality compared to COM902, we used a murine CD8⁺ T cell re-stimulation assay system. Activated OVA-specific CD8⁺ T cells were combined with a mPVR⁺ H-2 K^b cancer cell line (MC38) that had been pulsed with the OVA_(257–264) peptide. Expression of TIGIT and PD-1 on OVA-specific CD8⁺ T cells and PVR, PD-L1, and H2-K^b on MC38 cells is shown in Fig. 7a. Treatment with chimeric COM902 or anti-PD-L1 antibody alone led to enhanced IFN-γ secretion while the combination further increased IFN-γ release to 167% above the isotype control (Fig. 7b). To determine whether the observed effects of chimeric COM902 in-vitro translate in-vivo, we assessed the effect of COM902 on the colon carcinoma CT26 tumor model. Similar to the expression pattern we observed in dissociated human tumors (Fig. 1), mouse TIGIT was expressed on both T and NK lymphocytes isolated from CT26 tumors, with the highest expression found on CD4⁺ Tregs followed by CD8⁺ T_{EM} cells and NK cells (Fig. 7c, d). Additionally, PVR, PVRL2 and PD-L1 were abundantly expressed on the CD45⁺ cell population within CT26 tumors (Fig. 7e). Tumor bearing mice treated with the chimeric COM902 mIgG1 antibody as a single agent showed similar tumor growth and survival rates as compared to control groups (Fig. 8a, b, Supplementary Figure S3a). The combination of chimeric COM902 and anti-mPVRIG treatment resulted in a significant TGI and increase in overall survival compared to anti-PVRIG monotherapy (Fig. 8a). Similarly, combination of chimeric

COM902 and anti-PD-L1 resulted in significant TGI and enhanced overall survival compared to treatment with anti-PD-L1 monotherapy (Fig. 8b, Supplementary Figure S3a). We also evaluated the combination of chimeric COM902 and anti-mPVRIG using the Renca renal carcinoma tumor model. This model was selected since TIGIT, PVRIG, PVR and PVRL2 are expressed in Renca-tumor bearing mice (data not shown). The combination resulted in a significant TGI and an enhanced overall survival (Fig. 8c, Supplementary Figure S3b). Consistent with the low Fcγ receptor binding of a mIgG1 isotype and with the lack of ADCC and CDC activity of COM902 hIgG4 (Fig. 4), chimeric COM902 did not induce the depletion of tumor-infiltrating CD8⁺ T cells (Supplementary Figure S3c). Collectively, these results demonstrate the potential of COM902 in combination with anti-PVRIG or anti-PD-L1 to enhance anti-tumor lymphocyte responses and inhibit tumor growth in-vivo.

Discussion

The TME shapes the T cell dysfunctional state through a diverse stimuli, including TCR triggering in the absence of co-stimulation, chronic antigen exposure [24–26] and an altered milieu of secreted and metabolic factors [27]. TILs often display alterations in TCR signaling pathways, express a variety of inhibitory receptors and fail to produce effector molecules. TIGIT is a member of the immunomodulatory DNAM-1 axis that includes numerous immune receptors and ligands. Previous studies have demonstrated that TIGIT expression is highly associated with T cell exhaustion and marks activated, antigen-experienced, and dysfunctional T cells [10, 11, 28]. Correlation of TIGIT with PD-1 expression in human malignancies suggests that blockade of TIGIT binding to its cognate ligand, PVR, could synergize with anti-PD-(L)1 cancer treatment [10]. Recently, we identified and described the PVRIG pathway as a non-redundant negative signaling node within the DNAM axis that synergizes with TIGIT and PD-1 inhibitors [2]. Taken together, these findings support investigating the clinical rationale of combining TIGIT blockade with PVRIG and PD-1 inhibitors.

To evaluate TIGIT and PVR expression within the TME of human tumors, we utilized multi-color flow cytometry and IHC. TIGIT was expressed on CD4⁺, CD8⁺, and NK cells isolated from tumors, with the highest expression on CD4⁺ Tregs, which was consistent with other reports analyzing protein and single cell RNA data from various tumor indications [20, 28, 29]. Importantly, compared to matched NAT lymphocytes, TIGIT was markedly upregulated on TILs indicative of their exhausted state. We determined that PVR was expressed on CD45⁺ tumor and stroma cells as well as CD14⁺ myeloid cells (likely composed of tumor associated macrophages). The presence of elevated levels



of TIGIT on immune cells and abundant PVR expression across multiple tumor types on tumor cells and CD14⁺ TAMs indicates that this signaling pathway could be a pivotal mechanism for tumor evasion and provides the rationale for investigating effects of TIGIT blockade on immune modulation. In support of this hypothesis, previous studies have shown that PVR overexpression is closely correlated

with enhanced tumor progression and poor clinical outcomes [21, 30, 31]. We also noted that PVR expression was high in several healthy, normal tissues. Given that COM902 was well tolerated up to 100 mg/kg in cynomolgus monkeys in a repeat-dose GLP safety study (data not shown), and the favorable safety profile of anti-TIGIT mAbs in ongoing

Fig. 7 Chimeric COM902 enhances in-vitro anti-tumor activity of mouse T cells. **a** The expression of TIGIT and PD-1 on OT-1 splenocytes activated for 3 days with OVA_(257–264) peptide and rhIL-2, as well as of H-2K^b, PVR, and PD-L1 on MC38 target cells was assessed. Gray histograms represent the target staining and white histograms represent staining with the matched isotype control antibodies. Plots shown are from a representative experiment ($n=2$). **b** Mouse OVA-specific CD8⁺ T cells were co-cultured with OVA-peptide-pulsed MC38 cells in the presence of the chimeric COM902 as a monotherapy or in combination with PD-L1 blockade. The secretion of IFN- γ relative to isotype control is shown for each condition. Mean \pm SD are shown by the hash marks. **c** TIGIT expression on infiltrating lymphocytes isolated from s.c. CT26 tumors is shown as fold expression relative to the isotype control antibody (MFI_r) for each cell subset. Each dot represents an individual mouse ($n=3$) and mean \pm SEM. **d** Representative TIGIT expression on indicated cell populations from CT26 tumors. Blue, red, and gray histograms represent staining with COM902, chimeric COM902, and the mIgG1 isotype control, respectively. **e** PVR, PVRL2, and PD-L1 expression on CD45⁺ cells isolated from CT26 tumors. Gray histogram represents mIgG1 isotype control. Representative MFI_r values are reported to the right of each histogram

clinical trials, we do not foresee that the PVR expression profile in normal tissues will be toxicity concern.

Next, to assess the therapeutic potential of TIGIT blockade for the treatment of solid and hematological malignancies, we developed COM902, a fully human hinge-stabilized IgG4 mAb, that is specific for TIGIT and blocks its binding to human, cynomolgus, and mouse PVR. We selected an IgG4 isotype to minimize unintended Fc γ receptor-mediated cytotoxicity against TIGIT⁺ CD8⁺ TILs. As confirmed experimentally in CDC and ADCC assays, COM902 is unlikely to elicit direct cytotoxicity of TIGIT⁺ cells. The exceptionally high affinity and long off-rate of COM902 binding to human TIGIT, 626 fM and 2 days, respectively, as measured by Kinexa, could also offer significant clinical advantages. Due to the fact that lower clearance rates have been reported for antibodies with high affinity [32], COM902 may have a more significant biological effect at lower doses could be amenable to less frequent dosing compared to other TIGIT antibodies with lower binding affinities.

To study the effects of COM902 on human immune cell function, we carried out three in-vitro assays: a Jurkat reporter assay, an antigen-specific CD8⁺ T cell co-culture assay, and a NK cell cytotoxicity assay. We found that COM902 increased IL-2 signaling from Jurkat cells in a dose-dependent manner, suggesting that blockade of TIGIT and PVR binding by COM902 can enhance pro-inflammatory cytokine signaling. Prior studies have established that the properties of dysfunctional exhausted T cells are shared between cancer and chronic infection [27]. In particular, the expression of inhibitory receptors such as TIGIT, PVRIG, and PD-1 is upregulated on both CMV-specific effector cells and on TILs. Thus, our in-vitro assay system that utilizes

viral-specific CD8⁺ T cells is relevant for modeling T cell responses at the tumor and immune system interface.

The addition of COM902 to the co-cultures of CMV-specific CD8⁺ T cell and Mel-624 cells significantly increased IFN- γ secretion and target cell specific cytotoxicity. We and others have shown co-expression of PD-1, TIGIT and PVRIG on TILs [2, 10, 33, 34]. Accordingly, blocking TIGIT with COM902 combined with either PVRIG or PD-1 pathway blockade significantly induced IFN- γ secretion compared to blockade of each individual pathway alone. Furthermore, the presence of a fixed dose of anti-PVRIG or anti-PD-1 did not significantly change the EC₅₀'s for COM902, confirming that combining the inhibition of these non-redundant pathways should not alter the potency of COM902. Finally, we demonstrated that the co-blockade of TIGIT and PVRIG not only enhanced CD8⁺ T cell function, but also increased human NK cell cytotoxicity.

To determine if COM902 could also enhance the anti-tumor immune response in-vivo, we designed a chimeric COM902 with mIgG1 Fc, to maintain a minimal degree Fc γ receptor binding, similar to the hIgG4 antibody. Consistent with data generated with COM902 in human assay systems, chimeric COM902, both alone and in combination with anti-mouse PD-L1, increased in-vitro immune function of OVA-specific mouse CD8⁺ T cells. To evaluate the effect of chimeric COM902 in-vivo, we selected the CT26 and Renca syngeneic tumor models. Although monotherapy with chimeric COM902 did not show efficacy in either model, the combination of chimeric COM902 with anti-PD-L1 or anti-PVRIG both produced significant TGI and increased survival. The in-vivo results with chimeric COM902 are consistent with a recent study showing that treatment of MC38 tumor-bearing mice with the anti-TIGIT mIgG1 as a single agent had little anti-tumor responses, but when combined with an anti-PD-1 mIgG1 resulted in an 89% reduction in tumor growth in-vivo [35]. While other studies have shown robust anti-tumor activity of TIGIT blockade with effector mIgG2a backbone as a single agent as well as in combination with anti-PD-(L)1 in syngeneic mouse tumor models [10, 35], here we show significant TGI with a non-effector function anti-TIGIT mIgG1 antibody combined with a PD-L1 or PVRIG inhibitor. These data suggest that dual blockade of checkpoint receptors using therapeutic antibodies lacking effector function is required for sufficient activation and proliferation of CD8⁺ TILs in the TME. In addition, although studies with anti-TIGIT mIgG2a demonstrated monotherapy activity in-vivo, mouse models do not mirror the structural diversity and expression pattern of the human Fc receptor systems [36], and thus their translational relevance for human isotype selection is questionable, as exemplified by early clinical results with hIgG1 isotype anti-TIGIT antibodies. As we and others have shown, TIGIT is expressed on CD4⁺ Tregs, which suppress tumor immunity,

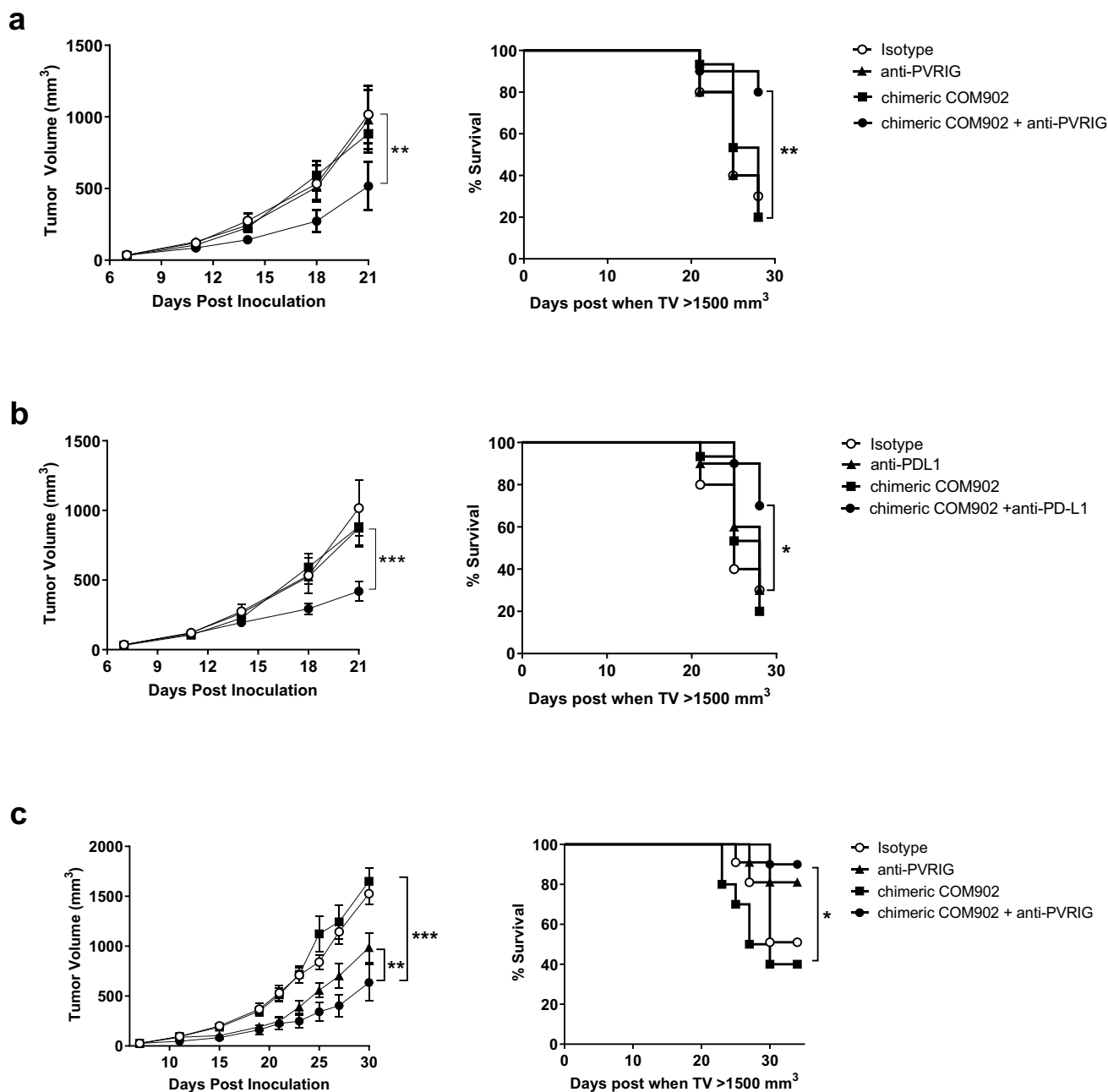


Fig. 8 Anti-tumor effect of chimeric COM902 in the CT26 and Renca tumor models as a single agent and in combination with anti-PVRIG or anti-PD-L1. BALB/c mice ($n=10$ mice per group) were s.c. injected with CT26 or Renca cells and dosed with the indicated antibodies starting from day 8 for combination therapies. Tumor volumes represented as the mean volume \pm SEM and Kaplan–Meier

survival curves are shown for the chimeric COM902 and anti-PVRIG combination in the CT26 model (a), the chimeric COM902 and anti-PD-L1 combination in the CT26 model (b), or the chimeric COM902 and anti-PVRIG combination in the Renca model (c). One representative experiment of $n \geq 2$ experiments for each combination is shown

as well as CD8⁺ effector T cells that mediate the anti-tumor immunity (Fig. 1). Given this overlap in TIGIT expression, an effector function TIGIT antibody, which has the potential to deplete Tregs, also carries the risk of depleting CD8⁺ TILs. For this reason, TIGIT antibodies with hIgG4 or hIgG1 effector silenced isotypes, such as COM902, would

not deplete CD8⁺ TILs and therefore may have an advantage over TIGIT antibodies with wild type hIgG1 backbones. Collectively, this study highlights the functional activity of COM902 and provides a strong rationale for combining COM902 with PD-1 or PVRIG blockade for the rejuvenation of the anti-tumor immune response and effective eradication

of human malignancies. Additional studies investigating the mechanism of action of TIGIT blockade as well as translational studies from ongoing clinical trials will be important to help further understand the factors that determine the biological effect and clinical efficacy of TIGIT inhibitors.

Supplementary Information The online version contains supplementary material available at <https://doi.org/10.1007/s00262-021-02921-8>.

Acknowledgement KH, SK, KL, SW, SQ, HYC, AD, MT, PW, DB, LL, EO, ZA, GC, MG, MF, MW, JH, SL and MK received salary from Compugen Ltd at the time of this study.

References

- Sharma P, Hu-Lieskovan S, Wargo JA, Ribas A (2017) Primary, adaptive, and acquired resistance to cancer immunotherapy. *Cell* 168:707–723. <https://doi.org/10.1016/j.cell.2017.01.017>
- Whelan S, Ophir E, Kotturi MF et al (2019) PVRIG and PVRL2 are induced in cancer and inhibit CD8 + T-cell function. *Cancer Immunol Res* 7:257–268. <https://doi.org/10.1158/2326-6066.CIR-18-0442>
- Stanietsky N, Simic H, Arapovic J et al (2009) The interaction of TIGIT with PVR and PVRL2 inhibits human NK cell cytotoxicity. *Proc Natl Acad Sci USA* 106:17858–17863. <https://doi.org/10.1073/pnas.0903474106>
- Yu X, Harden K, Gonzalez LC et al (2009) The surface protein TIGIT suppresses T cell activation by promoting the generation of mature immunoregulatory dendritic cells. *Nat Immunol* 10:48–57. <https://doi.org/10.1038/ni.1674>
- Shibuya A, Campbell D, Hannum C et al (1996) DNAM-1, a novel adhesion molecule involved in the cytolytic function of T lymphocytes. *Immunity* 4:573–581. [https://doi.org/10.1016/S1074-7613\(00\)70060-4](https://doi.org/10.1016/S1074-7613(00)70060-4)
- Shibuya K, Lanier LL, Phillips JH et al (1999) Physical and functional association of LFA-1 with DNAM-1 adhesion molecule. *Immunity* 11:615–623. [https://doi.org/10.1016/S1074-7613\(00\)80136-3](https://doi.org/10.1016/S1074-7613(00)80136-3)
- Chiang EY, de Almeida PE, de Almeida Nagata DE et al (2020) CD96 functions as a co-stimulatory receptor to enhance CD8+ T cell activation and effector responses. *Eur J Immunol* 50:891–902. <https://doi.org/10.1002/eji.201948405>
- Zhu Y, Paniccia A, Schulick AC et al (2016) Identification of CD112R as a novel checkpoint for human T cells. *J Exp Med* 213:167–176. <https://doi.org/10.1084/jem.20150785>
- Vaena D, Patnaik A, Hamilton E et al (2019) Abstract CT168: Phase I study of COM701 (a novel checkpoint inhibitor of PVRIG) in patients with advanced solid tumors. *Cancer Res*. <https://doi.org/10.1158/1538-7445.AM2019-CT168>
- Johnston RJ, Comps-Agrar L, Hackney J et al (2014) The immunoreceptor TIGIT regulates antitumor and antiviral CD8 + T cell effector function. *Cancer Cell* 26:923–937. <https://doi.org/10.1016/j.ccell.2014.10.018>
- Chauvin J, Pagliano O, Fourcade J et al (2015) TIGIT and PD-1 impair tumor antigen-specific CD8+ T cells in melanoma patients. *J Clin Invest* 125:2046–2058. <https://doi.org/10.1172/JCI80445>
- Harjunpää H, Guillerey C (2020) TIGIT as an emerging immune checkpoint. *Clin Exp Immunol* 200:108–119. <https://doi.org/10.1111/cei.13407>
- Alteber Z, Kotturi MF, Whelan S et al (2021) Therapeutic targeting of checkpoint receptors within the DNAM-1 axis. *Cancer Discov*, Accepted
- Golan T, Bauer TM, Golan T, et al (2018) Phase 1 dose-finding study of the anti-TIGIT antibody MK-7684 as monotherapy and in combination with pembrolizumab in patients with advanced solid. 33rd annual meeting and pre-conference programs of the society for immunotherapy of cancer (SITC 2018). *J Immunother Cancer* (SITC 2018). *J Immunother Cancer* 6:115 Abstract O25
- Sharma S, Ulahannan S, Mettu NB, et al (2018) Initial results from a phase 1a/b study of Etigilimab (OMP-313M32), an anti-T cell immunoreceptor with Ig and ITIM domains (TIGIT) antibody in advanced solid tumours. 33rd annual meeting and pre-conference programs of the society for immunotherapy of cancer (SITC 2018). *J Immunother Cancer* 6(Suppl 1) Abstract P289
- Bendell JC, Bedard P, Bang Y-J et al (2020) Phase Ia/Ib dose-escalation study of the anti-TIGIT antibody tiragolumab as a single agent and in combination with atezolizumab in patients with advanced solid tumors. *Cancer Res*. <https://doi.org/10.1158/1538-7445.AM2020-CT302>
- Rodriguez-Abreu D, Johnson ML, Hussein MA et al (2020) Primary analysis of a randomized, double-blind, phase II study of the anti-TIGIT antibody tiragolumab (tira) plus atezolizumab (atezo) versus placebo plus atezo as first-line (1L) treatment in patients with PD-L1-selected NSCLC (CITYSCAPE). *J Clin Oncol* 38:9503–9503. https://doi.org/10.1200/jco.2020.38.15_suppl.9503
- Finnefrock AC, Fu T-M, Freed DC, et al (2012) PD-1 Binding Proteins. U.S. Patent No. 8,168,757
- Murter B, Pan X, Ophir E et al (2019) Mouse PVRIG has CD8 + T cell-specific coinhibitory functions and dampens antitumor immunity. *Cancer Immunol Res* 7:244–256. <https://doi.org/10.1158/2326-6066.CIR-18-0460>
- Savas P, Virassamy B, Ye C et al (2018) Single-cell profiling of breast cancer T cells reveals a tissue-resident memory subset associated with improved prognosis. *Nat Med* 24:986–993. <https://doi.org/10.1038/s41591-018-0078-7>
- Sun Y, Luo J, Chen Y et al (2020) Combined evaluation of the expression status of CD155 and TIGIT plays an important role in the prognosis of LUAD (lung adenocarcinoma). *Int Immunopharmacol* 80:106198. <https://doi.org/10.1016/j.intimp.2020.106198>
- Liu W, Putnam AL, Xu-yu Z et al (2006) CD127 expression inversely correlates with FoxP3 and suppressive function of human CD4+ T reg cells. *J Exp Med* 203:1701–1711. <https://doi.org/10.1084/jem.20060772>
- Farhood B, Najafi M, Mortezaee K (2019) CD8 + cytotoxic T lymphocytes in cancer immunotherapy: a review. *J Cell Physiol* 234:8509–8521. <https://doi.org/10.1002/jcp.27782>
- Miller BC, Sen DR, Al AR et al (2019) Subsets of exhausted CD8+ T cells differentially mediate tumor control and respond to checkpoint blockade. *Nat Immunol* 20:326–336. <https://doi.org/10.1038/s41590-019-0312-6>
- Schietinger A, Philip M, Krisnawan VE et al (2016) Tumor-specific T cell dysfunction is a dynamic antigen-driven differentiation program initiated early during tumorigenesis. *Immunity* 45:389–401. <https://doi.org/10.1016/j.immuni.2016.07.011>
- Philip M, Schietinger A (2019) ScienceDirect heterogeneity and fate choice: T cell exhaustion in cancer and chronic infections. *Curr Opin Immunol* 58:98–103. <https://doi.org/10.1016/j.coi.2019.04.014>

27. Speiser DE, Ho P, Verdeil G (2016) Regulatory circuits of T cell function in cancer. *Nat Rev Immunol* 16:599–611. <https://doi.org/10.1038/nri.2016.80>
28. Yost KE, Satpathy AT, Wells DK et al (2019) Clonal replacement of tumor-specific T cells following PD-1 blockade. *Nat Med* 25:1251–1259. <https://doi.org/10.1038/s41591-019-0522-3>
29. Fourcade J, Sun Z, Chauvin JM et al (2018) CD226 opposes TIGIT to disrupt Tregs in melanoma. *JCI insight* 3:1–13. <https://doi.org/10.1172/jci.insight.121157>
30. Nishiwada S, Sho M, Yasuda S et al (2015) Clinical significance of CD155 expression in human pancreatic cancer. *Anticancer Res* 35:2287–2297
31. Stamm H, Oliveira-ferrer L, Grossjohann E et al (2019) Targeting the TIGIT-PVR immune checkpoint axis as novel therapeutic option in breast cancer. *Oncoimmunology* 8:e1674605. <https://doi.org/10.1080/2162402X.2019.1674605>
32. Leipold D, Prabhu S (2019) Pharmacokinetic and pharmacodynamic considerations in the design of therapeutic antibodies. *Clin Transl Sci* 12:130–139. <https://doi.org/10.1111/cts.12597>
33. Kurtulus S, Sakuishi K, Ngiow S et al (2015) TIGIT predominantly regulates the immune response via regulatory T cells. *J Clin Invest* 1:1–10. <https://doi.org/10.1172/JCI81187DS1>
34. Chihara N, Madi A, Kondo T et al (2018) Induction and transcriptional regulation of the co-inhibitory gene module in T cells. *Nature* 558:454–459
35. Han JH, Cai M, Grein J et al (2020) Effective anti-tumor response by TIGIT blockade associated with FcγR engagement and myeloid cell activation. *Front Immunol* 11:1–14. <https://doi.org/10.3389/fimmu.2020.573405>
36. Nimmerjahn F, Ravetch JV (2008) Fcγ receptors as regulators of immune responses. *Nat Rev Immunol* 8:34–47. <https://doi.org/10.1038/nri2206>

Publisher's Note Springer Nature remains neutral with regard to jurisdictional claims in published maps and institutional affiliations.